Tin(IV) Chalcogenide Complexes: Single Source Precursors for SnS, SnSe and SnTe Nanoparticle Synthesis.

Joseph R. Thompson,[a] Ibbi Y. Ahmet,[a] Andrew L. Johnson*[b] and Gabriele Kociok-Köhn[c]

Dedication ((optional))

Abstract: A family of tin(IV) *bis*-hexamethylsisylamide complexes **2-9** have been synthesized by reaction of [Sn{N(SiMe$_3$)$_2$}$_2$] (**1**) with the diphenyl dichalcogenanes Ph$_2$E$_2$ (E = S, Se, Te), the radical species TEMPO, or the group 16 elements to form the complexes [(PhE)$_2$Sn{N(SiMe$_3$)$_2$}$_2$] (**2**-**4**) and [(TEMPO)$_2$Sn{N(SiMe$_3$)$_2$}$_2$] (**5**), and [{(Me$_3$Si)$_2$N}$_2$Sn(μ^2-E)]$_2$ (**6**-**9**) (E = S, **2** & **6**; E = Se **3** & **7**; E = Te, **4** & **9,** E = O$_2$, **9**). The isolated tin complexes were characterized by elemental analysis, NMR spectroscopy, and the molecular structures of the complexes were determined by single crystal X-ray diffraction. Thermogravimetric analysis showed complexes **2**-**4** and **6**-**8** all to have residual masses close to those expected for the formation of the corresponding 'SnE' systems. Complexes **2**-**4** and **6**-**8** were also assessed for their utility in the formation of nanoparticles. The materials obtained were characterized by powder X-ray diffraction (XRD), field emission scanning electron microscopy (FE-SEM) and energy dispersive X-ray analysis (EDX). Analysis showed formation of SnSe and SnTe from complexes **3**-**4** and **6**-**7**, respectively.

Introduction

The *p*-type semiconducting tin(II) oxide and chalcogenide materials SnO, SnS, SnSe and SnTe all have the potential to be exploited in a range of applications including microelectronics, superconducting crystals, rechargeable batteries and solar cells because of their semiconductor properties and variable band gaps.[1] Apart from SnO (band gap = 2.82-2.97 eV), which is transparent to visible light,[2] the tin mono-chalcogenides 'SnE' (E = S, Se and Te) all have intense absorption across the electromagnetic spectrum, with narrow band gaps (E = S, 1.1 eV (direct), 1.3 eV (indirect); E = Se, 0.9 eV (direct), 1.3 eV (indirect); E = Te, 0.18 eV).[3] For optoelectronic applications, properties such as charge transfer and charge transport strongly depend on the morphology and crystallinity of the materials and whether the materials is a thin film or nanocrystals.[4] Literature over the past two decades shows quite clearly that the most critical and significant aspect of controlling the morphology of both thin films and nanocrystals is the selection of starting molecular precursors.[5] It is this selection that determines subsequent parameters such as choice of solvent and reaction temperature in the case of nanocrystal formation, and deposition procedure and deposition temperatures in the case of thin film chemical vapor deposition (CVD).[6]

Another important feature in the development of Sn(II) oxide and chalcogenide materials is the ability to control oxidation state, so as to suppress the production of higher oxidation state materials (i.e. Sn$_2$O$_3$, SnO$_2$, Sn$_2$S$_3$ SnS$_2$, Sn$_2$Se$_3$ and SnSe$_2$), the presence of which can be detrimental to the performance of binary Sn(II) oxide or chalcogenide materials.[1a,7] Therefore, the ability to control the formation of these materials is paramount, and to this end a large number of ligand systems have been developed.

We have recently reported the development of single source precursors based around the reaction of tin(II) *bis*(dimethylamide) with isocyanates and thioisocyanates respectively, which display unprecedented control of oxidation state in the production of both SnO[2, 8] and SnS materials.[7]

Amide ligand systems have been used extensively in the production of single source precursors for both thin film and nanoparticle production.[5a] While dialkyl amide ligands, such as {NMe$_2$}, are capable of stabilising selected M(II) species (e.g. [Sn{NMe$_2$}$_2$]$_2$), bulkier less electron rich amides such as {N(SiMe$_3$)$_2$} (HMDS) are significantly more capable of stabilizing low oxidation state M(II) species. The *bis*-HMDS complexes [Sn(II){N(SiMe$_3$)$_2$}$_2$] has found application in the direct synthesis of metal chalcogenide nanoparticles by reaction with chalcogenide transfer reagents (e.g. TOPO, TOPS, TOPSe and TOPTe)[9] in the presence of surfactants (e.g. olylamine or hexadecylamine).

Here, we report an investigation into the reactivity of [Sn{N(SiMe$_3$)$_2$}$_2$] with group 16 elemental species and oxidising group 16 reagents such as TEMPO and Ph$_2$E$_2$ (E = S, Se and Te), as well as their thermal decomposition profiles and application in nanoparticle synthesis.

Results and Discussion

In general, homoleptic chalcogenide complexes of otherwise unsaturated metal centres (e.g. Ge(II) and Sn(II) alkoxides and thiolates) have a tendency to form oligomeric or polymeric structures,[10] a result of which is that these complexes often have reduced solubility, high melting points and are non-

[a] J. R. Thompson and I. Y. Ahmet
Center for Sustainable Chemical Technologies
Department of Chemistry,
University of Bath. Claverton Down, Bath, BA2 7AY, UK.
[b] A. L. Johnson
Department of Chemistry,
University of Bath. Claverton Down, Bath, BA2 7AY, UK
E-mail: a.l.johnson@bath.ac.uk
[c] G. Kociok-Köhn
Chemical Characterisation and Analysis Facility (CCAF),
University of Bath. Claverton Down, Bath, BA2 7AY, UK

Supporting information for this article is given via a link at the end of the document.((Please delete this text if not appropriate))

volatile. This precludes their application in conventional CVD processes for which volatility is an important prerequisite for a precursor. One way in which the formation of these extended networks may be arrested is the use of kinetically stabilizing ligands on either the chalcogenide or the metal centre. In the case of Sn(II), the homoleptic stannylene complex $[Sn\{N(SiMe_3)\}_2]_2$ (**1**) reported independently in 1974, firstly by Zuckerman[11] and subsequently by Lappert[12] is an outstanding example of this concept. In both solution and the solid state **1** is monomeric, however the complex has both a free electron pair (nucleophilic centre) and an empty orbital (electrophilic centre) on the tin atom and labile strongly polarized Sn-N bonds which leads to a unique set of properties allowing **1** to participate in a range of oxidative addition reactions as well as ligand exchange reactions.

As such, a number of reports have been published on the reaction of stannylenes (R_2Sn), including **1**, with elemental chalcogenide species, which result in the formation of either complexes containing chalcogenide bridges, terminal Sn=E bonds or cyclic polychalcogenide materials.[13] In addition reaction of stannylenes R_2Sn with dichalcogenanes R'_2E_2 are known to result in the formation of complexes of the form $R_2Sn(ER')_2$ (E = S, Se or Te).[13a, 14]

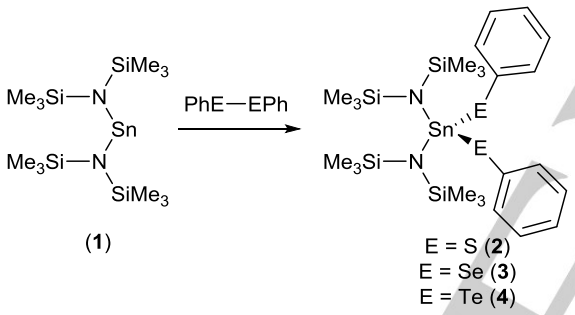

Scheme 1. Synthesis of complexes **2**-**4**.

Reaction of the stannylene **1** with one equivalent of diphenyl disulphide at ambient temperature results in an immediate colour change from yellow/orange to a deep orange colour and the quantitative formation (yield >80%) of the *bis*-phenylthiolate complex $[\{(Me_3Si)_2N\}_2Sn(SPh)_2]$ (**2**) (Scheme 1). Similarly, reaction of **1** with either diphenyl diselenide (Ph_2Se_2) or diphenyl ditelluride (Ph_2Te_2) respectively, also results in a rapid colour change and formation of the corresponding *bis*-phenylselenolate and *bis*-phenyltelluroate complexes, **3** and **4** respectively in yields over 90%. The identity of complexes **2**-**4** were authenticated by both NMR spectroscopy and single crystal X-ray diffraction analysis. Purity of the products was confirmed by elemental analysis of the products. Both **3** and **4** have been recently described by Sarizin el al.[14c] However, compound **3** reported here, is observed in a different polymorphic form to that previously reported.[14c] Data collected for compound **4** is, within experimental error, identical to that previously reported.[14c] As part of our discussion, relevant bond lengths and bond angles from our single crystal X-ray diffraction studies and relevant NMR data will be discussed.

Multinuclear NMR data for compounds **1**-**9** is summarized in table 1. ^1H and ^{13}C NMR spectra of the products (**2**-**4**) showed only the expected resonances due to the Phenyl and $\{N(SiMe_3)\}$ groups in the expected 1:1 ratios. Complexes **3** and **4** both display narrow singlet resonances in the $^{77}Se\{^1H\}$ and $^{125}Te\{^1H\}$ spectra respectively (Table 1), both with clearly distinguishable ^{117}Sn and ^{119}Sn satellites [**3**: $^1J_{Se\text{-}117Sn}$ = 1161 Hz, $^1J_{Se\text{-}119Sn}$ = 1168 Hz; **4**: $^1J_{Te\text{-}117Sn}$ = 4215 Hz, $^1J_{Te\text{-}119Sn}$ = 4424 Hz]. Complexes **2**-**4** also display single sharp resonances in the $^{119}Sn\{^1H\}$ NMR spectra moving progressively to lower ppm as the chalcogenide atom changes from S to Te and the relative electronegativities decreases (S>Se>Te).

Table 1. Selected NMR resonances (ppm) for **1**-**9**.

	Cord.^{N} No.	$\delta^{119}Sn$	$\delta^{77}Se$	$\delta^{125}Te$
$[Sn\{N(SiMe_3)_2\}_2]$[15] (**1**)	2	776		
$[(PhS)_2Sn\{N(SiMe_3)_2\}_2]$ (**2**)	4	-70		
$[(PhSe)_2Sn\{N(SiMe_3)_2\}_2]$ (**3**)	4	-183	206	
$[(PhTe)_2Sn\{N(SiMe_3)_2\}_2]$ (**4**)	4	-443		288
$[(TEMPO)_2Sn\{N(SiMe_3)_2\}_2]$ (**5**)	4	-100		
$[\{(Me_3Si)_2N\}_2Sn(\mu^2\text{-}S)]_2$ (**6**)	4	-105		
$[\{(Me_3Si)_2N\}_2Sn(\mu^2\text{-}Se)]_2$ (**7**)	4	-381	397	
$[\{(Me_3Si)_2N\}_2Sn(\mu^2\text{-}Te)]_2$ (**8**)	4	-986		749
$[\{(Me_3Si)_2N\}_2Sn(\mu^2\text{-}O_2)]_2$ (**9**)	4	-266		

Single crystals of compounds **2**-**4** were obtained upon cooling (-25 °C) of freshly prepared hexane solutions. All three complexes are isostructural albeit over different space groups; **2** and **3** crystalize in the space group P-1 (**3** was reported by Sarizin el al.[14c] in a monoclinic form), whereas **4** crystallises here, in the monoclinic space group C2/c. The molecular structure of **2** shows the Sn atom to exist within a pseudo tetrahedral coordination environment (Fig. 1).

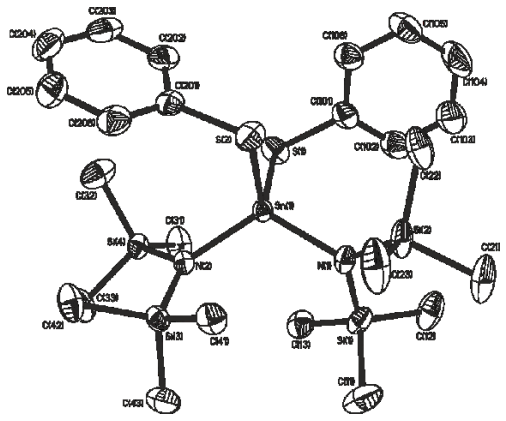

Figure 1. The asymmetric unit of **2** showing the labelling scheme used; ellipsoids are at the 50% probability level. Hydrogen atoms have been omitted for clarity.

Not unsurprisingly the average Sn-E bond length [av. 2.4148(15) Å (**2**), 2.5469(15) Å (**3**) and 2.7673(3) Å (**4**)] increase with the increasing atomic number of the chalcogenide atom, and are in good agreement with both comparable Sn-E single bonds within the Cambridge Structural Database (CSD), specifically the related ethylchalcogenane compounds [{$(Me_3Si)_2N$}$_2$Sn$(EEt)_2$] described by Schulz *et. al.* and theoretical values for single bonds calculated from the sum of the single bond covalent radii.[14d]

Table 2. Selected bond distances (Å) and angles (°) for **1**-**4**

	Sn-N	Sn-E	N-Sn-N	E-Sn-E	N-Sn-E
1[a]	2.088(6) 2.096(1)		104.7(2)		
2[b]	2.0482(15) 2.0460(14)	2.4224(5) 2.4072(5)	116.87(6)	107.41(2)	108.82(4) 105.43(5) 107.19(4) 110.77(4)
3[b]	2.053(3) 2.058(3)	2.5456(5) 2.5483(5)	114.17(12)	106.344(17)	110.44(9) 109.76(9) 110.02(8) 105.72(9)
4[b]	2.063(3)	2.7673(3)	112.21(16)	108.895(15)	109.95(7) 107.90(7)

[a] taken from [15]. [b] This work.

As can be seen in Table 2 the Sn-N bond-lengths for **2**-**4** are all significantly shorter than the corresponding bond-lengths in the parent complex **1** [av. 2.091(6) Å] and become progressively longer with the increasing atomic number of the chalcogenide atom. Following the same trend, the N-Sn-N bond angles also increase with the chalcogenide atom, contrasting with the ethyl derivatives, within which the N-Sn-N bond angles remain between approx. 113-112° irrespective of the {E-Et} group coordinated to the tin centre.[14d]

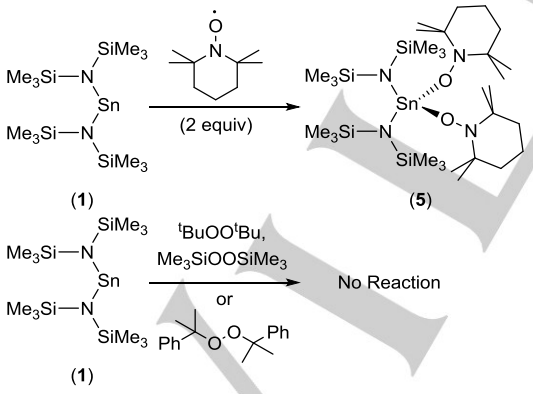

Scheme 2. Attempted reaction of **1** with peroxide species and the synthesis of complex **5**

While the oxidative addition of species such as the dichalcogenides, e.g. PhE-EPh (E= S, Se or Te), to divalent group 14 complexes is relatively commonplace, comparable reaction with the lightest congener of this family (i.e PhO-OPh) is unknown, by virtue of the non-existence of PhO_2Ph. However, peroxides such ^{t}BuOO^{t}Bu and $Me_3SiOOSiMe_3$ are known and have been reported to react with divalent Group 14 species such as silylene and germylene complexes respectively, via the *in-situ* formation of the corresponding tert-Butoxy or trimethylsiloxy radicals.[16]

Attempts to react the stannylene **1** with peroxides were partly successful: reaction of **1** with ^{t}BuOO^{t}Bu resulted in an immediate formation of a white and intractable material. Reaction of **1** with the either the bis(trimethylsilyl)peroxide or dicumyl peroxide showed now obvious reactivity and attempts to recrystallize products resulted in isolation of the stannylene 1. Gratifyingly, reaction of **1** with two equivalents of the stable oxygen radical species TEMPO resulted in an almost instantaneous extinction of the red colour associated with TEMPO and concomitant formation of a clear yellow solution. On cooling of the concentrated reaction mixture (-28 °C) yellow crystals formed, which were isolated and analysed by single crystal X-ray diffraction. The heteroleptic Sn(IV) complex [{$(Me_3Si)_2N$}$_2$Sn$(TEMPO)_2$] (**5**) can be clearly seen in Figure 2 and comprises of two TEMPOxide ligands unambiguously bound to the central tin atom in an terminal fashion through the oxygen atom. Two HMDS groups, {$N(SiMe_3)$}, complete the coordination environment about the *pseudo*-tetrahedral tin atom. Both the Sn-N and Sn-O bond lengths are consistent with other Sn(IV) complexes both in this study and beyond.

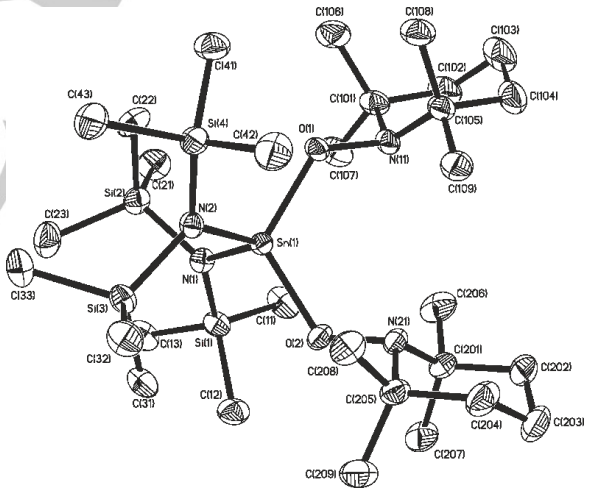

Figure 2. The asymmetric unit of **5** showing the labelling scheme used; ellipsoids are at the 50% probability level. Hydrogen atoms have been omitted for clarity.

Analysis of the bond lengths in **5** clearly show a lengthening on the {O-N} bonds in the TEMPOxide ligands and an a significant pyramidalization of the nitroxide-nitrogen atom indicative of single electron reduction of the radical starting material and formation of the Sn(IV) complex.[18]

^{1}H and ^{13}C NMR spectra for **5** showed only the expected resonances due to TEMPOxide and {$N(SiMe_3)$} groups in the anticipated 1:1 ratios. Complexes **5** also display single sharp resonances in the ^{119}Sn{^{1}H} NMR at δ= -100; between the δ^{119}Sn shifts observed for compounds **2** and **3**. Peak broadening,

indicative of the presence of radical contaminants were not observed in any of the spectra collected. TEMPO radicals have previously been shown to react with the cyclic silylene, germylene and stannylene systems in a stepwise fashion *via* an intermediary metal mono TEMPOxide radical, the formation of which is slow compared to its reaction with a second equivalent of TEMPO to form the stable *bis*-TEMPOxide systems.[16b, 17] While in solution (NMR) there is no evidence of the radical intermediate (**5·**), exposure of a solid sample of **5** to a vacuum, at room temperature over a period of time, does result in the sublimation of what we identify as small amounts of TEMPO, suggesting the reaction to form **5** from the stannylene **1** is reversible. Single electron transfer (SET) products similar to **5·** have recently been identified as potentially σ-bond metathesis catalysts.[18]

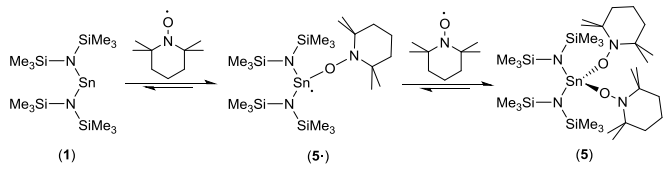

Scheme 3. Reversible stepwise SET reaction of **1** with TEMPO to form **5**.

While the reaction of **1** with TEMPO can be seen to be reversible, the contrasting reaction of the cyclic stannylene, [Sn{C(SiMe$_3$)$_2$CH$_2$CH$_2$C(SiMe$_3$)}] with TEMPO to form the *bis*-TEMPOxide complex [(TEMPO)$_2$Sn{C(SiMe$_3$)$_2$CH$_2$CH$_2$C(SiMe$_3$)}] show no such reversibility.[17a] This difference presumably arises from dissimilarities in the steric and electronic environment about the two Sn-centres. In the case of the cyclic stannylene, reaction of the highly strained sp^2 Sn(II) centre [C-Sn-C = 86.7(2)° *Cf* 120°], with TEMPO, results in formation of a significantly less strained sp^3 sn(IV) centre [C-Sn-C = 90.85(7)° *Cf* 109.5°].[17a] This relief of strain for the cyclic system presumably makes the reverse reaction unfavourable. In contrast whilst a comparable widening of the N-Sn-N [**1**: 104.7(2) °; **5**: 110.36(6) °] bond angle is also observed on oxidation of **1** to **5**, any relief of strain at the Sn centre is considerably less. The flexibility of the HMDS ligands allows for a much wider O-Sn-O angle [**5**: 117.67 °; cf. 112.66(6) °].

Interestingly, **5** shows very limited thermal stability: heating of either solid or solutions of **5** results in rapid decomposition from which tractable products could not be isolated. It was initially hoped that such decomposition pathways could be a potential route to the oxide bridged system [{(Me$_3$Si)$_2$N}$_2$Sn(μ^2-O)]$_2$, via the cleavage of the N-O of putative radical **5·**,·and subsequent 'SnO' precursors.

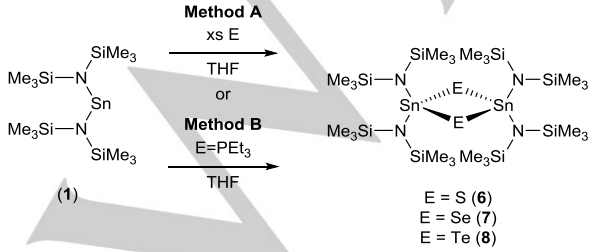

Scheme 4. Synthesis of complexes **6**-**8** using method A and method B.

The oxidative addition of chalcogenides and chalcogenide donor reagents with stannylenes is well known.[13a, 13c, 13f, 14b] Direct reaction of two equivalents of the elemental chalcogenides S, Se or Te results in the formation of the binary Sn(IV) chalcogenide complexes [{(Me$_3$Si)$_2$N}$_2$Sn(μ^2-E)]$_2$ (E = S, Se or Te) (**6**-**8**) as yellow to red crystalline compounds as previously reported by Lappert *et al.*[13f] The same materials can be synthesised by reaction with the chalcogenide transfer reagents R$_3$P=S, R$_3$P=Se and R$_3$P=Te (R = Et or Ph) respectively. However, reaction with the triphenyl phosphine derivatives made purification of the products problematic, as residual Ph$_3$P was difficult to remove from the reaction mixture.

The ^{1}H and ^{13}C NMR spectra of compounds **6**-**8** showed only the expected resonances due to the and {N(SiMe$_3$)} groups. However complexes **7** and **8** both display narrow singlet resonances in the ^{77}Se{^{1}H} and ^{125}Te{^{1}H} spectra respectively (Table 2), both with clearly distinguishable ^{119}Sn and ^{117}Sn satellites [**7**: $^2J_{119Sn-117Sn}$ = 566 Hz, $^1J_{77Se-119Sn}$ = 1130 Hz, $^1J_{77Se-117Sn}$ = 1127 Hz; **8**: $^1J_{125Te-117Sn}$ = 2651 Hz, $^1J_{Te-119Sn}$ = 2746 Hz]. Complexes 6-8 also display single sharp resonances in the ^{119}Sn{^{1}H} NMR spectra which move progressively to lower ppm as the chalcogenide atom changes from S to Te (*Cf.* **2**-**4**).

As part of our study we re-collected single crystal diffraction data for complexes **6**-**8** at 150K. The complexes **6**-**8** are isostructural and each comprise of central 4-membered planar ring of alternating tin and chalcogenide atoms, with two {N(SiMe$_3$)$_2$} ligands coordinated to each tin atom. For completeness, and comparison to other structures in this report, figure 3 shows the molecular structure of 8 (representative of complexes **6**-**8**) and table 3 provides selected bond lengths and bond angles.

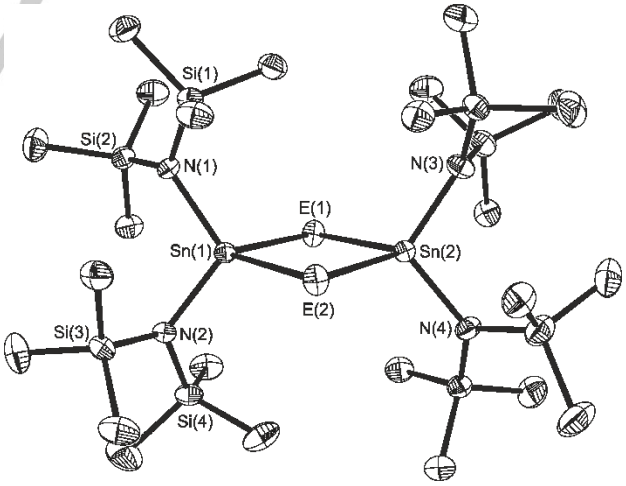

Figure 3. Figure Molecular structure of [{(Me$_3$Si)$_2$N}$_2$Sn(μ^2-Te)]$_2$ (**8**), ellipsoids are at the 50% probability level. Hydrogen atoms have been omitted for clarity. Labelling scheme for **6** (E = S) is identical to **8**; for **7** (E= Se) the atoms E(2), Sn(2), N(3) and N(4) etc. are generated by an inversion centre at the centre of the {Sn$_2$E$_2$} ring. Symmetry operator: [-X, -Y, -Z].

Table 3. Selected bond distances (Å) and angles (°) for 6-8.

	Sn-E	Sn-N	E-Sn-E	N-Sn-N	Sn-E-Sn
6 (E=S)	2.4262(6) 2.4140(6) 2.4142(6) 2.4162(6)	2.042(2) 2.046(2) 2.040(2) 2.036(2)	93.16(2) 93.41(2)	114.65(8) 112.87(8)	86.597(18) 86.823(19)
7 (E=Se)	2.5357(3) 2.5469(3)	2.051(2) 2.057(2)	95.105(9)	110.08(9)	84.895(9)
8 (E=Te)	2.7544(4) 2.7482(4) 2.7534(4) 2.7596(4)	2.053(3) 2.061(3) 2.055(3) 2.061(3)	96.826(11) 96.581(11)	108.89(13) 106.93(14)	83.226(10) 83.227(10)
9 (E=O_2)[a]	2.001(2) 1.999(2) 2.002(2) 1.999(2)	2.015(2) 2.011(2) 2.012(2) 2.015(2)	99.65(8) 99.57(8)	121.77(9) 122.63(9)	

[a]: O-O distances 1.512(2)Å and 1.506(3)Å.

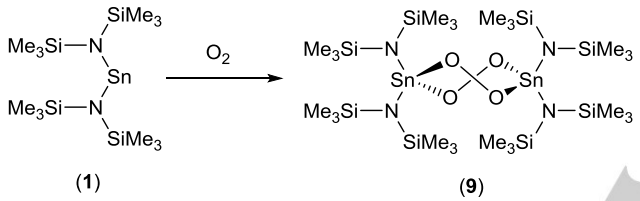

(**1**) (**9**)

Scheme 5. Reaction of **1** with dioxygen to form **9**.

Unlike its heavier congeners, reaction of Et_3PO (Or Ph_3PO) with **1** does not result in oxygen transfer to the Sn centre, presumably because of the greater P=O bond strength, compared to P=S, P=Se and P=Te. NMR spectra ($^{31}P\{^1H\}$ and $^{119}Sn\{^1H\}$) of the reaction mixture revealed the presence of only starting materials. Reaction of **1** with dioxygen gas yields the *bis*(1,2-μ-peroxo)-bridged species (**9**) (Scheme.5), initially reported by Lappert *et al.* in 1992.[19] Surprisingly, the reaction between **1** and O_2 appears to be insensitive to both thermal activation and photo activation (irradiation with 254-185nm light source) failed to yield either the oxide analogue of complexes **6-8**, *i.e.* $[\{(Me_3Si)_2N\}_2Sn(\mu^2\text{-}O)]_2$ or the ozinide complex $[\{(Me_3Si)_2N\}_2Sn(\mu^2\text{-}O_2)(\mu^2\text{-}O)]_2$, both of which have been reported for the related *bis*(trimethylsilyl)methyl, $\{(Me_3Si)_2CH\}$, containing complexes.[13f, 20]

As with complexes **6-8** the ^1H and ^{13}C NMR spectra of the product (**9**) showed only the $\{N(SiMe_3)\}$ resonances. The ^{119}Sn NMR spectrum shows a single resonance at δ = -266 ppm which is between ^{119}Sn resonances for the S and Se complexes (**7** and **8**) respectively.

Thermogravimetric Analysis

Thermogravimetric analysis (TGA) was performed on compounds **2-9** to study their decomposition patterns in an attempt to ascertain their potential utility as single-source precursors. The TGA traces of the related compounds **2-5** and **6-9**, respectively are shown in Figures 5 and 6 with the tabulated data shown in Table 4.

In the case of the *bis*-phenylchalcogenide systems **2-4** we observe relatively clean single stepped decomposition pathways; for the sulfur and selenium derivatives, **2** and **3** respectively, mass loss is initiated at temperatures of approx. 200 °C. In contrast, the tellurium derivative **4**, which also appears to undergo a single step decomposition event, experiences the onset of decomposition at the much lower temperature of 143 °C. In all three cases the final residual mass is significantly less than expected mass for the formation of the respective 'SnE' compound, indicating a significant degree of volatility in the precursors, which may make them suitable for various CVD applications.

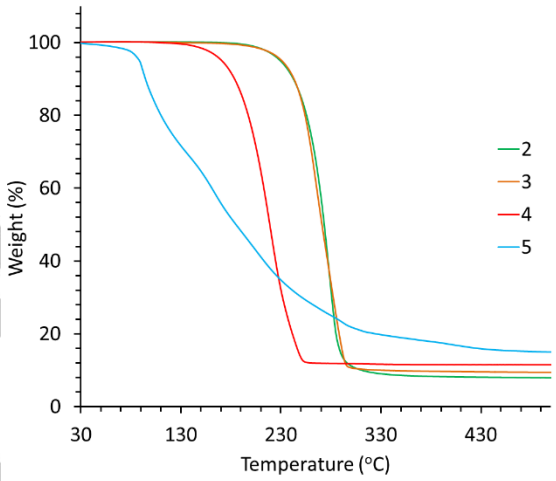

Figure 4. TGA Data for complexes **2-5**.

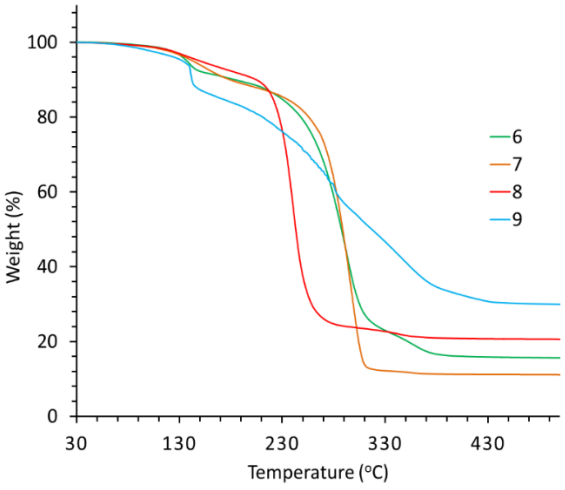

Figure 5. TGA Data for complexes **6-9**.

In stark contrast to compounds **2**-**4**, the TEMPOxide derivative **5** displays a very shallow decomposition profile with initial mass loss beginning at approx. ~79 °C and levelling out to a constant mass at 435 °C, the final residual mass being significantly higher (~30.5 %) than the calculated residues expected for SnO (18%).

For compounds **6**-**9**, all three systems possess similar decomposition onset temperatures of ≤100 °C, as well as similar 1st stage small mass losses of 6-11 % between 100 and 200 °C, followed by a more rapid 2nd mass loss [**6**: ~240 °C; **7**: ~250 °C; **8**: ~210 °C]. As with **2**-**4**, complexes **6**-**8** all show residual masses less than expected for the formation of the corresponding SnE system, again highlighting the potential application of these systems in CVD processes.

Table 4. Summary of TGA data for compounds **2** - **9**.

Compound	Onset / °C	End point /°C	% Wt. Expected for SnE	Final %Wt.
2	202	345	23	8.7
3	198	302	26	10.6
4	143	255	29	12.1
5	79	435	18	30.5
6	100	388	32	16.3
7	93	325	38	12.3
8	96	368	43	21.1
9	58	495	29	15.0

In contrast, **9**, with a complicated decomposition profile shows progressive mass loss between a onset temperature of 58 °C and 495 °C leaving a mass residue of 15% (significantly below the mass % expected for SnO formation) again indicative of possible volatility of the precursor. However the complex decomposition profile and high temperature at which mass loss terminates, may make complex **9** an unsuitable CVD precursor.

Tin chalcogenide Nanocrystals

In a typical procedure for the preparation of tin chalcogenide nanocrystals, the precursor was dissolved in a minimum volume of hexane. To this solution oleylamine was added and the hexane was removed *in vacuo*. The reaction mixture was then heated at 210 °C for 40 mins before being allowed to cool to room temperature. Excess ethanol was added and the precipitate was collected by ethanol washing and centrifugation three times. The tin chalcogenide precursors **2**-**4** and **6**-**8**, were used in the nanocrystal preparation procedure with varying degrees of success: Both compounds **5** and **9** failed to make identifiable monocrystalline oxide materials.

As part of our initial studies the *bis*-phenylselenide complex, **3**, was reacted with olylamine at 210 °C for 20 mins, 40 mins and 2 hours respectively. After workup the resulting nanoparticles were analysed by TEM, the images of the resulting particles are shown in figure 6. The particles produced over the three time periods varied considerably in size between *ca.* 60 – 90 nm (20mins), 0.5 – 1.0 µm (40 mins) and 250 – 500 nm (120 mins).

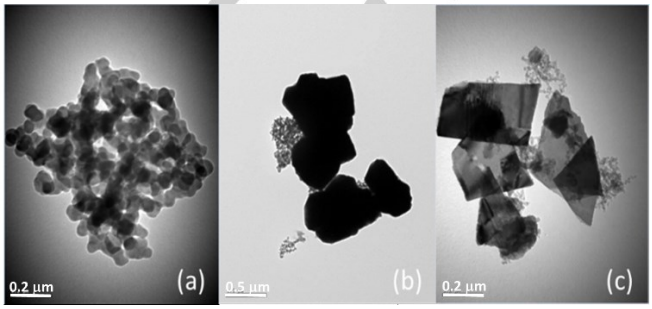

Figure 6: TEM images of the 'SnSe' particles made from **3**, (a) 20 mins (0.2µm), (b) 40 mins (0.5µm) and (c) 2 hours (0.5µm).

EDX analysis also showed a variation in composition with respect to reaction time. While analysis showed the presence of both Sn and Se in the appropriate quantities for materials synthesised over both the 40 mins reaction time (1:1 At%, Sn:Se ratio) and 2 hours reaction time (1:0.98 At%, Sn:Se ratio) (figure 7), materials produce with a short 20 mins reaction time appeared to be Se rich (1:1.34 At%, Sn:Se ratio) (EDX spectra can be seen in the ESI): Suggesting that a reaction time of 20 mins was too short a time for complete decomposition and formation of the desired tin chalcogenides to have taken place.

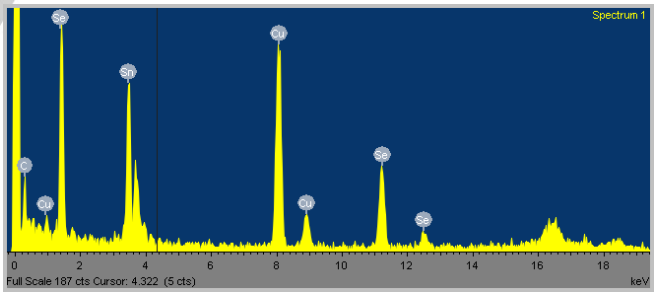

Figure 7: EDX spectrum of the 'SnSe' nanoparticles produced from precursor **3** after 40 mins reaction time. Cu peaks in the spectra result from the underlying copper mesh used as a support.

Electron diffraction patterns were observed for the particles produced over both 40 mins and 2 hours suggesting the particles are crystalline. However, for the material produced with a 20 mins reaction time no electron diffraction pattern was observed.

In an identical procedure, particles produced from the bridged seleno-complex, **7**, appear in the SEM micrograph to be

star shaped clusters *ca.* 200 – 300 nm in size (Figure 8). Despite the outward contrast in morphology EDX analysis suggest formation of SnSe, with a nearly stoichiometric ratios of Sn:Se (1:1 and 1.04:1) for nanocrystals formed from **3** and **7** respectively. PXRD analysis of the nanomaterials produced from both complex (**3** and **7**) match data reported for the orthorhombic SnSe (Pnma) (JCPDS #481224).[9b]

The particles produced from the *bis*-phenyltelluride complex (**4**) with a 40 min reaction time were globular and encased within what appears to be a large organic thin film structure (Figure 9a). These particles possess a large variation in sizes at *ca.* 10 – 100 nm. The EDS spectrum (Figure 9b) showed the particles to be Sn rich with a Sn:Te ratios of 1.1:1. No electron diffraction pattern was observed suggesting the particles were amorphous. In contrast, particles produced from the bridged telluride complex, **8**, displayed a range of shapes and sizes: the large particle shown in Figure 11a was measured at *ca.* 1.9 µm by 1.3 µm, whilst the smaller particles on top of the larger particle were measured at *ca.* 350 by 350 nm. The hexagonal particle in Figure 11b has a diameter of *ca.* 250 nm.

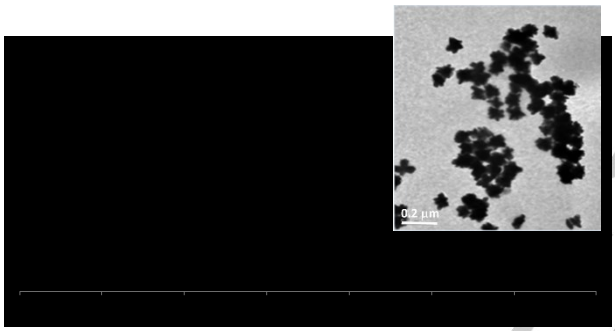

Figure 8. PXRD pattern of the 'SnSe' nano-particals made from **7**; TEM images (inset) of the 'SnSe' particles (0.2µm) made from **7**.

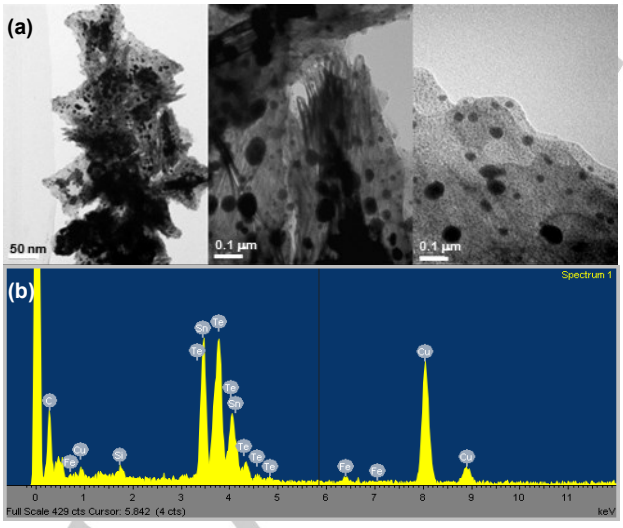

Figure 9. (a) Nanoparticles produced from precursor **4**, encased in a thin film structure. (b) EDX spectrum of the nanoparticles produced from precursor 4.

The EDX analysis showed the nanoparticles produced from **8** to be slightly Sn rich with a Sn:Te ratios of 1.17:1, a facet which seems to be common of nanocrystals of SnTe, compared to bulk SnTe which typically Sn-deficient.[21] Traces of Si were observed suggesting either some starting material remains or silicon containing by-product may be present. An electron diffraction pattern indicates the presence of crystalline material; a PXRD pattern of the particles is shown in figure 10 and corresponds to the cubic Fm3m structure of SnTe (JCPDS #652945), highlighting the successful preparation of SnTe from precursor **8**.[9c, 21]

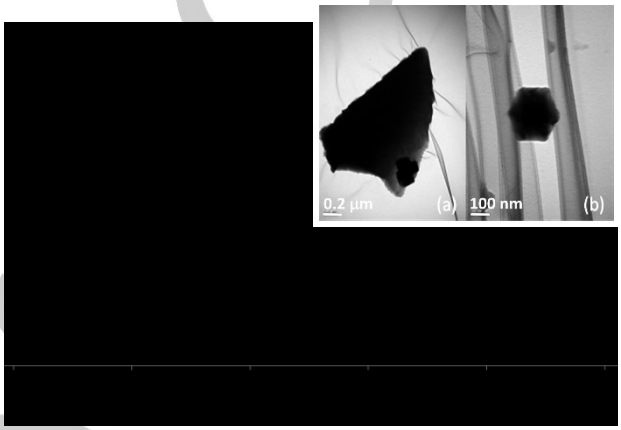

Figure 10. PXRD pattern of the 'SnTe' nanoparticles made from **8**; TEM images (inset) of the 'SnTe' particles (**a**: 0.2µm, **b**: 100 nm) made from **8**.

The materials produced from precursors **2** and **6** appear to be agglomerates of smaller particles (See ESI). While EDX analysis showed the presence of both Sn and S with a Sn:S ratio of 3.3:1, traces of O and Si were also present, suggesting either contamination by insoluble O and Si containing by-products or possible oxidation of the 'SnS' nanoparticles. While an electron diffraction pattern was observed suggesting the particles were crystalline, PXRD data was inconclusive showing only very broad low intensity reflections indicative of small particle size.

Conclusions

This work documents the synthesis and characterisation of a family of tin (IV) *bis*-hexamethyldisilazide complexes, **2-9**, as potential precursors for the production of tin(II) chalcogenide materials. The synthetic procedure for the production of the tin complexes is straight forward and the products can be isolated in good yields and easily scaled-up. The molecular structure of eight complexes (**2-9**) have been determined revealing the tin centres to possess four coordinate *pseudo*-tetrahedral coordination environments. TGA shows the thermal properties of complexes **2-4** and **6-8** to be encouraging with respect to exploitation as single source tin chalcogenide precursors, possessing relatively clean decomposition characteristics, and residual masses indicative of the formation of the corresponding 'SnE' materials (E = S, Se and Te). For the oxygen containing Sn(IV) complexes (**5** and **9**) the TG analyses display more complicated decomposition pathways; TGA of complex **5**

produces residual masses in excess of that expected for SnO, whereas complex **9** produces residual masses less than that expected for SnO production. More significantly however, the inherent instability of these complexes renders them unlikely precursors. As part of our study we chose to examine the potential of these systems as single source precursor for nanoparticle formation (un-optimised). For both the SnSe and SnTe nanoparticles (synthesised from precursors **3**/**7** and **4**/**8** respectively) XRD and EDX provide clear evidence of formation of the desired SnE materials. Our future efforts in this area are directed at optimizing nanoparticle formation and controlling both morphology and size of the nanoparticles, as well as investigating these materials for other CVD thin film applications

Experimental Section

General Procedures: Elemental analyses were performed using an Exeter Analytical CE 440 analyser. ^{1}H, ^{13}C ^{119}Sn, ^{77}Se and ^{125}Te NMR spectra were recorded on a Bruker Advance 300 or 500 MHz FT–NMR spectrometers, as appropriate, as saturated solutions at room temperature, unless stated otherwise; chemical shifts are in ppm with respect to Me_4Si (^{1}H, ^{13}C). TGA and PXRD were performed using a Perkin Elmer TGA7 or Bruker D8 instrument (Cu-k_α radiation), respectively.

All reactions were carried out under an inert atmosphere using standard Schlenk techniques. Solvents were dried and degassed under an argon atmosphere over activated alumina columns using an Innovative Technology solvent purification system (SPS). The Sn(II) amide, [Sn{N(SiMe$_3$)$_2$}] (**1**), was prepared by literature method[15]; The reagents Ph_2S_2 Ph_2Se_2 Ph_2Te_2, TEMPO, S_8, Se, Te and Et_3P were purchased from Aldrich chemicals. The phosphines Et_3P=E (E = S, Se or Te) were synthesized via a modification of a literature method[22] and used as stock solutions (in toluene) of known molarity. The characterization data presented here for complexes **3**-**4** and **6**-**9** are consistent with those reported elsewhere.[13f, 14c, 19]

Synthesis of [{(Me$_3$Si)$_2$N}$_2$Sn(SPh)$_2$] (2)

Under inert conditions, bis[bis(trimethylsilyl)amido]tin(II) (2.20 g, 5 mmol) and phenyl disulfide (1.09 g, 5 mmol) were dissolved in THF (20 ml). After stirring for 3 hours the solution was dried in vacuo to provide an orange solid. The solid was extracted with hot hexane, and filtered through Celite™. Concentration and storage of the filtrate at -28 °C yielded the orange crystals which were isolated by filtration and dried in vacuo. Yield: 2.67 g, 97 %. ^{1}H NMR (300 MHz, C_6D_6) δ 0.34 (s, 36H, CH3), 7.03 (m, 6H, CH-aryl), 7.72 (m, 4H, CH-aryl); ^{13}C NMR (75 MHz, C_6D_6) δ 6.8, 128.5, 129.5, 131.4, 137.3; ^{119}Sn NMR (186.5 MHz, C_6D_6) δ -70; Elemental analysis (expected): C,43.85 (43.82); H, 6.88 (7.05), N, 4.34 (4.26); Melting point = 136 °C.

Synthesis of [{(Me$_3$Si)$_2$N}$_2$Sn(SePh)$_2$] (3)

Compound **4** was synthesised under identical conditions to compound **3** using 2.20 g of bis[bis(trimethylsilyl)amido]tin(II) (5 mmol) and 1.56 g of diphenyl diselenide (5 mmol).Yield: 2.86 g, 89 %; ^{1}H NMR (300 MHz, C6D6) δ 0.35 (s, 36H, CH3), 7.00 (m, 6H, CH-aryl), 7.76 (m, 4H, CH-aryl); ^{13}C NMR (75 MHz, C_6D_6) δ 6.9, 126.0, 128.8, 129.6, 139.0; ^{77}Se NMR (95 MHz, C_6D_6) δ 205, ^{1}J(^{77}Se-^{117}Sn) = 1611 Hz, ^{1}J(^{77}Se-^{119}Sn) = 1687 Hz; ^{119}Sn NMR (186.5 MHz, C_6D_6) δ -183, ^{1}J(^{119}Sn-^{77}Se) = 1688 Hz; Elemental analysis (expected): C, 38.51 (38.35); H 6.04 (6.17); N, 3.80 (3.73); Melting point = 134 °C.

Synthesis of [{(Me$_3$Si)$_2$N}$_2$Sn(TePh)$_2$] (4)

Under inert conditions 0.44 g of **1** (1 mmol) and diphenyl ditelluride (0.41 g, 1 mmol) were dissolved in THF (20 ml). After stirring for 3 hours the solution was dried in vacuo to provide an orange solid. The solid was extracted with hot hexane, and filtered through Celite™. Concentration and storage of the filtrate at -28 °C yielded the red/orange crystals which were isolated by filtration and dried in vacuo. Yield: 0.60 g, 81 %; ^{1}H NMR (300 MHz, C6D6) δ 0.38 (s, 36H, CH3), 6.90 (t, 4H, CH-aryl), 7.02 (t, 2H, CH-aryl), 7.88 (d, 4H, CH-aryl); ^{13}C NMR (75 MHz, C_6D_6) δ 7.2, 129.3, 129.9, 143.0; ^{119}Sn NMR (186.5 MHz, C_6D_6) δ -442, ^{1}J(^{119}Sn-^{125}Te) = 4423 Hz; ^{125}Te NMR (158 MHz, C_6D_6) δ 287, ^{1}J(^{125}Te-^{117}Sn) = 4215 Hz, ^{1}J(^{125}Te-^{119}Sn) = 4415 Hz; Elemental analysis (expected): C, 33.86 (33.96); H, 5.34 (5.46), N 3.40 (3.30); Melting point = 145 °C

Synthesis of [{(Me$_3$Si)$_2$N}$_2$Sn(TEMPO)$_2$] (5)

Under inert conditions, a hexane (10 ml) solution of **1** (0.88 g, 2 mmol) was added to a stirring hexane (10 ml) solution of 2,2,6,6-tetramethyl-1-piperidinyloxy (TEMPO) (0.62 g, 4 mmol), an immediate colour change from orange to a golden yellow was observed. After stirring for 2 hours the solution was dried in vacuo to provide a yellow solid. Extraction of the solid into hexane followed by filtration through celite™ and storage at -28 °C, yielded yellow crystals. Crystals of **5** were isolated by filtration, dried under vacuum and stored at -20 oC to avoid rapid decomposition. Yield: 1.10 g, 73 %; ^{1}H NMR (300 MHz, C_6D_6) δ 0.30 (s, CH_3), 0.56 (s, CH_3-TEMPO), 1.28 (s, CH_2-TEMPO), 1.58 (s, CH_2-TEMPO); ^{13}C NMR (75 MHz, C_6D_6) δ 3.0, 6.1, 8.10, 18.0, 21.8, 35.0, 41.8, 61.3; ^{119}Sn NMR (186.5 MHz, C_6D_6) δ -100; Elemental analysis (expected): C, 47.84 (47.92); H, 9.72 (9.65); N, 7.35 (7.45); Melting point = 79 °C

Method A: Synthesis of [{Sn[N(SiMe$_3$)$_2$]$_2$(μ-S)}$_2$] (6) using Elemental S.

Under inert conditions, sulfur powder (0.16 g, 0.63 mmol) and **1** (2.20 g, 5 mmol) were dissolved in THF (20 ml). After 2 hours of sonication the reaction mixture was heated at 60 °C for 48 hours. The reaction mixture was filtered through Celite™, and the filtrate reduced in volume and stored at -28 °C. Colourless crystals of **6** were isolated by filtration and dried in vacuo. Yield: 1.80 g, 76 %; ^{1}H NMR (300 MHz, C_6D_6) δ 0.48 (s, CH_3); ^{13}C

NMR (75 MHz, C_6D_6) δ 7.0 ; ^{119}Sn NMR (186.5 MHz, C_6D_6) δ -105, $^2J(^{119}Sn\text{-}^{117}Sn)$ = 610 Hz Elemental analysis (expected): C – 30.44 (30.57), H – 7.83 (7.70), N – 5.86 (5.94) Melting point = dec. ~218 °C.

Method B: Synthesis of [{Sn[N(SiMe$_3$)2]$_2$(μ-S)}$_2$] (6) using Et$_3$PS.

Under inert conditions, a toluene solution of Et_3PS (6.25 ml, 0.8 M, 5 mmol) was added to 2.20 g of **1** (5 mmol) dissolved in THF (20 ml). After stirring and gentle heating overnight the reaction mixture was filtered through Celite™, and the filtrate reduced in volume and stored at -28 °C. Colourless crystals of **6** were isolated by filtration and dried in vacuo. Yield: 1.53 g, 65%. The product displayed identical analysis to that produced using method A.

Synthesis of [{Sn[N(SiMe3)2]$_2$(μ-Se)}$_2$] (7).

Using method A compound **7** was synthesised under identical conditions to compound **6** using selenium powder (0.39 g, 5 mmol). Yield: 2.10 g, 81 %; ^{1}H NMR (300 MHz, C_6D_6) δ 0.49 (s, CH3); ^{13}C NMR (75 MHz, C_6D_6) δ 7.25; ^{77}Se NMR (95 MHz, C_6D_6) δ 398, $^1J(^{77}Se\text{-}^{117}Sn)$ = 1030 Hz, $^1J(^{77}Se\text{-}^{117}Sn)$ = 1127 Hz; ^{119}Sn NMR (186.5 MHz, C_6D_6) δ -381, $^2J(^{119}Sn\text{-}^{117}Sn)$ = 784 Hz; Elemental analysis (expected): C, 27.66 (27.80), H, 6.88 (7.00), N, 5.50 (5.40); Melting point = dec. ~148 °C.

Using method B, compound **7** was synthesised under identical conditions to compound **6** using a toluene solution of Et_3PSe (10ml, 0.5 M, 5 mmol). Yield: 1.76 g, 68 %. The product displayed identical analysis to that produced using method A.

Synthesis of [{Sn[N(SiMe$_3$)$_2$]$_2$(μ-Te)}$_2$] (8)

Using method A: Synthesised using tellurium powder (0.64 g, 5 mmol).Yield: 2.60 g, 92 %; ^{1}H NMR (300 MHz, C_6D_6) δ 0.52 (s, CH_3); ^{13}C NMR (75 MHz, C_6D_6) δ 7.58; ^{125}Te NMR (157 MHz, C_6D_6) δ 749, $^1J(^{125}Te\text{-}^{117}Sn)$ = 2651 Hz, $^1J(^{125}Te\text{-}^{119}Sn)$ = 2746 Hz; ^{119}Sn NMR (186.5 MHz, C_6D_6) δ -987, $^2J(^{119}Sn\text{-}^{117}Sn)$ = 566 Hz; Elemental analysis (expected): C, 25.59 (25.42); H, 6.46 (6.40); N, 4.88 (4.94); Melting point = dec. ~150 °C.

Using Method B: using a freshly prepared toluene solution of Et_3PTe (25ml, 0.2 M, 5 mmol). Yield: 2 g, 71 %. The product displayed identical analysis to that produced using method A.

Synthesis of [{Sn[N(SiMe$_3$)$_2$]$_2$(μ-O$_2$)}$_2$] (9)

A hexane solution (60 ml) of **1** (0.88 g, 2 mmol) stirred vigorously under an atmosphere of oxygen gas until a colour change was observed. After one hour the solvent was removed under reduced pressure. The white residue was extracted with hexane (20 ml) and filtered through celite™. The colourless filtrate was reduced in volume. Storage at -28 °C, yielded colourless crystals which were isolated by filtration dried in vacuo. Yield: 0.75 g, 60 %; ^{1}H NMR (300 MHz, C_6D_6) δ 0.45 (s, CH_3); ^{13}C NMR (75 MHz, C_6D_6) δ 5.9; ^{119}Sn NMR (112 MHz, C_6D_6) δ -266; Elemental analysis (expected): C,30.39 (30.57); H, 7.61 (7.70), N, 5.85 (5.94). Melting point = dec. ~110 °C.

General preparation of tin chalcogenide nanoparticles from precursors 2, 3 4, 6, 7, 8 and 9.

Under inert conditions, excess dry oleylamine (20 ml) was added to a hexane (10 ml) solution of the tin chalcogenide precursor (0.5 mmol). The hexane was removed in vacuo. The reaction mixture was heated at 210 °C for 40 mins (16 also heated for 20 mins and 2 hours). Once cooled to room temperature, excess ethanol was added. The precipitate was collected by centrifugation then purified by ethanol washing and centrifugation a further three times. The powder was dried in vacuo.

Crystallography

Experimental details relating to the single-crystal X-ray crystallographic studies are summarised in Tables S1 and S2 (ESI). Crystallographic data were collected at 150 K on a Nonius Kappa-CCD Diffractometer [$\lambda(Mo_{k\alpha})$ = 0.71073 Å], and solved by direct methods (SIR-92)[23] and refined against all F^2 using SHELXL–97.[24] All hydrogen atoms are included in idealised positions and refined using the riding model. Structure solution was followed by full-matrix least squares refinement and was performed using the WinGX-1.70 suite of programmes. All non-hydrogen atoms were refined anisotropically. CCDC 1489251-1489258 contains the supplementary crystallographic data for this paper. These data can be obtained free of charge at www.ccdc.cam.ac.uk/conts/retrieving.html [or from the Cambridge Crystallographic Data Center, 12, Union Road, Cambridge CB2 1EZ, UK; fax: +44-1223/336-033; E-mail: deposit@ccdc.cam.ac.uk].

Materials Chemistry

Thermogravimetric analyses (TGA) were obtained using a Perkin Elmer TGA 4000 analyser. Data points were collected every second at a ramp rate of 10 $^oC\ min^{-1}$ in a flowing (90 mL min^{-1}) N_2 stream.

FE-SEM analysis of the films was undertaken on a JEOL JSM-6480LV scanning electron microscope with EDX capability. AFM analysis was carried out on a Nanosurf Flexafm easyscan 2 instrument with a Tap 190 AL/G AFM tip and 10nm tip radius, (Tapping mode). Powder XRD of the films was performed on a Bruker D8 Powder Diffractometer, using a Cu anode X-ray source, (Kα wavelength = 1.5406 Å) at the University of Bath.

Acknowledgements

We thank EPSRC for funding (EP/L0163541 and EP/G03768X/1) and the Doctoral Training Centre in Sustainable Chemical Technologies (I.Y.A and J.R.T)

Keywords: Tin amide • Chalcogenide • single source precursor • TGA • nanoparticle.

References

[1] a) D. J. Lewis, P. Kevin, O. Bakr, C. A. Muryn, M. A. Malik, P. O'Brien, *Inorganic Chemistry Frontiers* **2014**, *1*, 577; b) Z. Wang, P. K. Nayak, J. A. Caraveo-Frescas, H. N. Alshareef, *Adv. Mater.,* **2016**, *28*, 3831-3892.

[2] T. Wildsmith, M. S. Hill, A. L. Johnson, A. J. Kingsley, K. C. Molloy, *Chem Commun.,* **2013**, *49*, 8773-8775.

[3] O. Madelung, *Semiconductors: Data Handbook*, Springer, Berlin ; London, **2004**.

[4] a) A. de Kergommeaux, J. Faure-Vincent, A. Pron, R. de Bettignies, B. Malaman, P. Reiss, *J. Am. Chem. Soc.,* **2012**, *134*, 11659-11666; bY. Yin, A. P. Alivisatos, *Nature,* **2005**, *437*, 664-670.

[5] a) M. Yarema, R. Caputo, M. V. Kovalenko, *Nanoscale,* **2013**, *5*, 8398; b) D. V. Talapin, J.-S. Lee, M. V. Kovalenko, E. V. Shevchenko, *Chem. Rev.,* **2010**, *110*, 389-458.

[6] P. Marchand, C. J. Carmalt, *Coord. Chem. Rev.,* **2013**, *257*, 3202-3221.

[7] I. Y. Ahmet, M. S. Hill, A. L. Johnson, L. M. Peter, *Chem. Mater.,* **2015**, *27*, 7680-7688.

[8] I. Barbul, A. L. Johnson, G. Kociok-Kohn, K. C. Molloy, C. Silvestru, A. L. Sudlow, *Chempluschem,* **2013**, *78*, 866-874.

[9] a) S. G. Hickey, C. Waurisch, B. Rellinghaus, A. Eychmüller, *J. Am. Chem. Soc.,* **2008**, *130*, 14978-14980; b) W. J. Baumgardner, J. J. Choi, Y.-F. Lim, T. Hanrath, *J. Am. Chem. Soc.,* **2010**, *132*, 9519-9521; c) M. V. Kovalenko, W. Heiss, E. V. Shevchenko, J. S. Lee, H. Schwinghammer, A. P. Alivisatos, D. V. Talapin, *J. Am. Chem. Soc.,* **2007**, *129*, 11354-11345.

[10] a) M. F. Lappert, P. P. Power, A. R. Sanger, R. C. Srivastava, *Metal and Metalloid Amides : Syntheses, Structures, and Physical and Chemical Properties*, E. Horwood, Chichester, **1980**; b) M. F. Lappert, A. Protchencko, P. P. Power, A. Seeber, *Metal Amide Chemistry*, Wiley, Oxford, **2009**.

[11] C. D. Schaeffer, J. J. Zuckerman, *J. Am. Chem. Soc.,* **1974**, *96*, 7160-7162.

[12] D. H. Harris, M. F. Lappert, *J. Chem. Soc., Chem. Commun.* **1974**, 895-896.

[13] a) P. B. Hitchcock, E. Jang, M. F. Lappert, *J. Chem. Soc., Dalton Trans.* **1995**, 3179-3187; b) M. K. Barman, S. Nembenna, *RSC Adv.* **2016**, *6*, 338-345; c) S. R. Foley, G. P. A. Yap, D. S. Richeson, *Organometallics,* **1999**, *18*, 4700-4705; d) S. M. Mansell, C. A. Russell, D. F. Wass, *Dalton Trans.,* **2015**, *44*, 9756-9765; e) M. Saito, N. Tokitoh, R. Okazaki, *J. Am. Chem. Soc.,* **1997**, *119*, 11124-11125; f) J. J. Schneider, J. Hagen, O. Heinemann, J. Bruckmann, C. Krüger, *Thin Solid Films,* **1997**, *304*, 144-148; g) Y. Zhou, D. S. Richeson, *J. Am. Chem. Soc.,* **1996**, *118*, 10850-10852.

[14] a) P. B. Hitchcock, M. F. Lappert, L. J. M. Pierssens, A. V. Protchenko, P. G. H. Uiterweerd, *Dalton Trans.,* **2009**, 4578; b) S. R. Foley, G. P. A. Yap, D. S. Richeson, *J. Chem. Soc., Dalton Trans.,* **2000**, 1663-1668; c) A. Pop, L. Wang, V. Dorcet, T. Roisnel, J.-F. Carpentier, A. Silvestru, Y. Sarazin, *Dalton Trans.,* **2014**, *43*, 16459-16474; d) G. Bendt, S. Lapsien, P. Steiniger, D. Bläser, C. Wölper, S. Schulz, *Z. Anorg. Allg. Chem.,* **2015**, *641*, 797-802.

[15] T. Fjeldberg, H. Hope, M. F. Lappert, P. P. Power, A. J. Thorne, *J. Chem. Soc., Chem. Comm.,* **1983**, 639-641.

[16] a) E. Bonnefille, S. Mazières, N. El Hawi, H. Gornitzka, C. Couret, *J. Organomet. Chem.,* **2006**, *691*, 5619-5625; b) A. Naka, N. J. Hill, R. West, *Organometallics,* **2004**, *23*, 6330-6332.

[17] a) T. Iwamoto, H. Masuda, S. Ishida, C. Kabuto, M. Kira, *J. Am. Chem. Soc.,* **2003**, *125*, 9300-9301; b) T. Iwamoto, H. Masuda, S. Ishida, C. Kabuto, M. Kira, *J. Organomet. Chem.,* **2004**, *689*, 1337-1341; c) B. Tumanskii, P. Pine, Y. Apeloig, N. J. Hill, R. West, *J. Am. Chem. Soc.,* **2004**, *126*, 7786-7787; d) B. Tumanskii, P. Pine, Y. Apeloig, N. J. Hill, R. West, *J. Am. Chem. Soc.,* **2005**, *127*, 8248-8249.

[18] a) D. J. Liptrot, P. M. S. Hill, M. F. Mahon, *Angew. Chem. Int. Ed. Engl.* **2014**, *53*, 6224-6227; b) P. Jochman, D. W. Stephan, *Chem Commum.,* **2014**, *50*, 8395-8397; c) K. Bundy-Godleweski, D. Kubicki, I. Justyniak, J. Lewiński, Organometallics, 2014, 33, 5093-5096.

[19] R. W. Chorley, P. B. Hitchcock, M. F. Lappert, *J. Chem. Soc., Chem. Commun.* **1992**, *0*, 525-526.

[20] a) M. A. Edelman, P. B. Hitchcock, M. F. Lappert, *J. Chem. Soc., Chem. Commun.* **1990**, 1116-1118; b) C. J. Cardin, D. J. Cardin, M. M. Devereux, M. A. Convery, *J. Chem. Soc., Chem. Commun.* **1990**, 1461-1462.

[21] S. Guo, A. F. Fidler, K. He, D. Su, G. Chen, Q. Lin, J. M. Pietryga, V. I. Klimov, *J. Am. Chem. Soc.,* **2015**, *137*, 15074-15077.

[22] C. M. Evans, M. E. Evans, T. D. Krauss, *J. Am. Chem. Soc.,* **2010**, *132*, 10973-10975.

[23] A. Altomare, G. Cascarano, C. Giacovazzo, A. Guagliardi, M. C. Burla, G. Polidori, M. Camalli, *J. Appl. Cryst.,* **1994**, *27*, 435-436.

[24] G. M. Sheldrick, *Acta Crystallogr. A,* **2008**, *64*, 112-122.

Entry for the Table of Contents (Please choose one layout)

Layout 1:

FULL PAPER

A family tin(IV) *bis*-HMDS complexes baring chalcogenide ligands have been synthesized and characterized. Selected complexes have been assessed for their utility in the formation of nanoparticles. Analysis (PXRD, SEM and EDS) showed formation of SnSe and SnTe respectively.

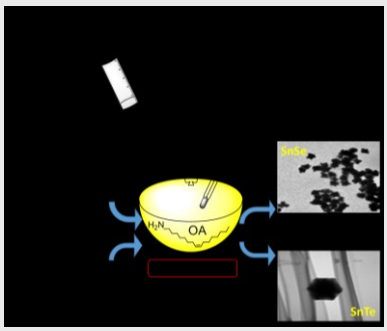

Key Topic Tin Chalcogenide Precursors

Joseph R. Thompson, Ibbi Y. Ahmet, Andrew L. Johnson and Gabriele Kociok-Köhn**

Page No. – Page No.

Tin(IV) Chalcogenide Complexes: Single Source Precursors for SnS, SnSe and SnTe Nanoparticle Synthesis

*one or two words that highlight the emphasis of the paper or the field of the study